Indonesian Journal of Earth Sciences, Vol. 05, No. 1 (2025), A1398

P-ISSN: 2798-1134 | E-ISSN: 2797-3549 | DOI: 10.52562/injoes.2025.1398

MO.RI Publishing

Indonesian Journal of Earth Sciences

InJoES

https://journal.moripublishing.com/index.php/injoes

| Research Article |

Check for updates

Flood Inundation Mapping and Spatial Analysis: A Case Study of the 2022 Massive Flood in Swat, Khyber Pakhtunkhwa, Pakistan

Atta Ullah[1,2], Saddique Akbar[1,2], Muhammad Afan Ghani[3], Muhammad Paryal[1,2], Muhammad Maaz[4], Noman Ali Shah[5], Imtiaz Momand[6]

[1]State Key Laboratory of Tibetan Plateau Earth System, Environment and Resources (TPESER), Institute of Tibetan Plateau Research, Chinese Academy of Sciences, Beijing 100080, China
[2]University of Chinese Academy of Sciences, Beijing 100049, China
[3]University of Engineering and Technology, Peshawar 54890, Pakistan
[4]Department of Environmental Sciences, Faculty of Biological Sciences, Quaid-i-Azam University, Islamabad 45320, Pakistan
[5]State Environmental Protection Key Laboratory of Wetland Ecology and Vegetation Restoration, School of Environment, Northeast Normal University, Changchun 130117, China
[6]Pakhtunkhwa Energy Development Organization (PEDO) KPK, Peshawar, Pakistan
**Correspondence: saddique@itpcas.ac.cn*

Received: 06 December 2024 / Accepted: 15 June 2025 / Published: 28 June 2025

Abstract: Climate change has increased the frequency of extreme precipitation, increasing rapid flood risks globally. This study integrates remote sensing, geospatial data and climatic statistics to map flood inundation and analyze precipitation patterns in Swat district, Khyber Pakhtunkhwa, Pakistan, following the 2022 flood. We used Google Earth Engine (GEE), applied supervised classification on sentinel-2 imagery achieving an accuracy of 99.7% for 2021 and 97.3% for 2022, confirming the precision of our analysis. Flood water body levels were meticulously scrutinized, culminating in the production of an illuminating flood inundation map through the Summer Permanent Water Bodies (SPWB) exclusion layer and Normalized Difference Flood Index (NDFI) framework. The NDVI and SPWB exclusion layer identified 1230 km^2 of inundated area and 258 km^2 of land use change in 2022. Analysis of Climate Hazards Group InfraRed Precipitation with Station (CHIRPS) summer precipitation data revealed a peak of 877 mm in 2022, with significant increase in southern, central and northern parts of Swat. This study is an earnest attempt to advance our understanding of flood mapping and offer roadmap for enhanced disaster management, supporting urban planning and mitigation strategies in the flood prone regions of Swat.

Keywords: Flood, Swat, Climate change, Inundation

INTRODUCTION

The frequency of extreme weather events has significantly increased globally due to the warming climate (Lehmann et al., 2015). Climate Change (CC) is leading to an increase frequency and intensity of extreme precipitation (EP) events and associated hazards (Zhang et al., 2021). CC is a challenge for agriculture, food security and rural livelihoods of billions of people all over the world (Kawo et al., 2021). Floods have become a global issue and are one of the most serious natural disasters worldwide (Sarhadi et al., 2012). Floods pose significant threats to human lives, livelihoods, properties and socio-cultural heritage (Billa et al., 2006; Liu et al., 2023; Rentschler et al., 2022; Samanta et al., 2018; Shen et al., 2022). Over the past 30 years, global data reveals that floods have affected an average of 80 million people annually (Dereli et al., 2021; Sakurai & Murayama, 2019). Over the past 40 years, floods have caused global damages exceeding $1 trillion USD (UNDRR, 2020). From 1994 to 2004, Asia experienced nearly 60,000 deaths due to natural catastrophes caused by overflow threats (Díez-Herrero & Garrote, 2020). The increase in major flood disasters over the past three decades has been a significant indicator of CC (Sarkar & Mondal, 2019; Tariq et al., 2022). Flooding is a significant global issue causing over 2,000 deaths annually and impacting over 75 million people in various ways (Abbas et al., 2023; Rentschler et al., 2022; Zou et al., 2013). Disasters in South Asia are most significantly affecting developing countries due to their increased vulnerability and exposure (Owusu et al., 2019). Every catastrophic event further pushes these nations on the verge of living down (Mahto & Mishra, 2019).

South Asian countries are notably impacted by summer monsoon floods, which significantly harm their lives and livelihoods (Almazroui et al., 2020). Over 1 billion people in South Asia have been affected by floods in the past 20 years, with extreme floods expected to increase due to climate change (Mirza, 2011). The Hindukush Himalaya (HKH) region experiences significant vulnerability due to frequent floods during the rainy season (Akbar et al., 2024; Tsering et al., 2022; Uddin et al., 2021).

The region has a history of severe floods, causing significant socioeconomic and physical damage (Khan et al., 2022). In 2010, the monsoon system caused severe rainfall, leading to devastating floods in Swat tributaries, destroying everything in its path (Butt et al., 2020). A deadly water surge in a mountainous region destroyed infrastructure, human settlements, buildings, cropped lands, irrigation networks, highways, and bridges, making communication inaccessible and causing widespread destruction (Farooq et al., 2019). The 2010 floods displaced 2,751 families, damaged 988 houses, and damaged 26 water channels in the region (Butt et al., 2020). On 29 August 2020, a heavy rainfall-induced flash flood in the Shagram torrent of Swat resulted in the deaths of at least 14 people, damages to 45 houses, and over 3 bridges (Nasir et al., 2020).

To address the increasing frequency of flood events and their devastating impact in Swat and other Himalayan regions, this study adopts a hybrid methodology integrating remote sensing and statistical analysis. The Normalized Difference Flood Index (NDFI) is selected as it enhances with the Summer Permanent Water Bodies (SPWB) exclusion layer, grounded in recent advancements in flood detection accuracy. Previous studies (e.g., Xue et al., 2022) demonstrated that NDFI alone can misclassify permanent water bodies as flood-affected zones. By combining SPWB, a more reliable classification of flood extent is achieved, particularly in riverine and lake-dense terrains. Google Earth Engine (GEE) was selected for its cloud-based computational capability, real-time access to Sentinel-2 imagery, and seamless integration of climatic and geospatial datasets. This enabled precise multi-temporal classification at a 10m resolution. Supervised classification using Random Forest offers robust classification performance, as evidenced by high kappa scores (>97%), and is known for outperforming traditional classifiers in heterogeneous environments such as Swat Valley (Cian et al., 2018; Alam et al., 2018). This framework thus provides a scalable, accurate, and computationally efficient solution for flood inundation mapping in mountainous regions. This paper examines the spatial land use changes in Swat using Google Earth Engine and the Supervised Classification random forest algorithm. The dataset, selected in 2021 and 2022, was classified with an average accuracy of 98% and a kappa coefficient of 97.5%, revealing the impact of massive floods on land use land cover. The Summer Permanent Water Bodies (SPWB) exclusion layer was used to extract flood inundation data. This study followed Xue et al. (2022) framework by combining the normalized difference flood index (NDFI) and the SPWB exclusion layer, with the main objective of inundation mapping using NDFI, and the change detection during one year due to flood. Flooding is a prevalent and destructive natural hazard causing global economic issues, necessitating accurate monitoring to understand its causes and potential solutions.

Study Area

Swat division located in Northern Pakistan, 34° 36′ 0″ and 34° 58′ 48″ north latitudes and 72° 0′ 0″ and 72° 35′ 24″ east longitudes an elevation between 733-5638 m.a.s.l. covering an area of 5215 km^2. Its northern parts are covered in high snow-covered mountains, while the southern part is plain with croplands along the riverbank. The Swat Valley experiences short summers and long winters, with annual rainfall ranging from 700 to 1630 mm (Malik & Ahmad, 2014). The high-altitude northern region experiences precipitation patterns influenced by winter snowfall from the Mediterranean Sea (Rebi et al., 2023; Ullah et al., 2020), whereas, the lower southern region is dominated by summer monsoon rainfall (Khan et al., 2020; Ullah et al., 2021). Low winter temperatures promote snow and glacier accumulation, while high summer temperatures trigger the melting of snow and glaciers (Chen et al., 2023; Huang et al., 2023). Study Area Map shown in Figure 1.

Pakistan experiences frequent floods during summer monsoon and occasionally tropical cyclones due to heavy precipitation (Paulikas & Rahman, 2015). The recent catastrophic flooding events in Pakistan serve as a stark reminder of the effects of climate change (Khan et al., 2022; Shah et al., 2023). Between 1950 and 2020, the country experienced 25 devastating floods, resulting in over 9,088 deaths and an estimated loss of 20 billion USD (Ahmed et al., 2023; Khan et al., 2021). In 2010, Pakistan experienced one of its most devastating floods due to severe monsoon precipitation, causing significant damage across the country (Farooq et al., 2019; Gaurav et al., 2011). A massive earthquake in Pakistan, affecting 20 million people across 78 districts and resulting in 1,985 deaths, caused an estimated 9.7 billion USD economic loss (Ahmed et al., 2023; Ullah et al., 2021). Pakistan is among the most severely affected nations by climate change, undergoing severe hydrometeorological events (Abbas et al., 2022;

Akbar et al., 2024; Baqa et al., 2022; Bhatti et al., 2020). The northern provinces of Pakistan are most severely impacted by floods in the upper tributaries of the Indus basin due to glacial melt and heavy rainfall (Paulikas & Rahman, 2015). The 2010 and 2022 floods severely affected northern and southern provinces in the country, with extreme precipitation causing flooding in the northern reaches of the Indus River, subsequently impacting the southern parts (Atta ur & Khan, 2013; Nanditha et al., 2023). The flood plains of Khyber Pakhtunkhwa, southern Baluchistan, and Sindh were severely impacted by the massive population (Yaqub & Eren, 2015).

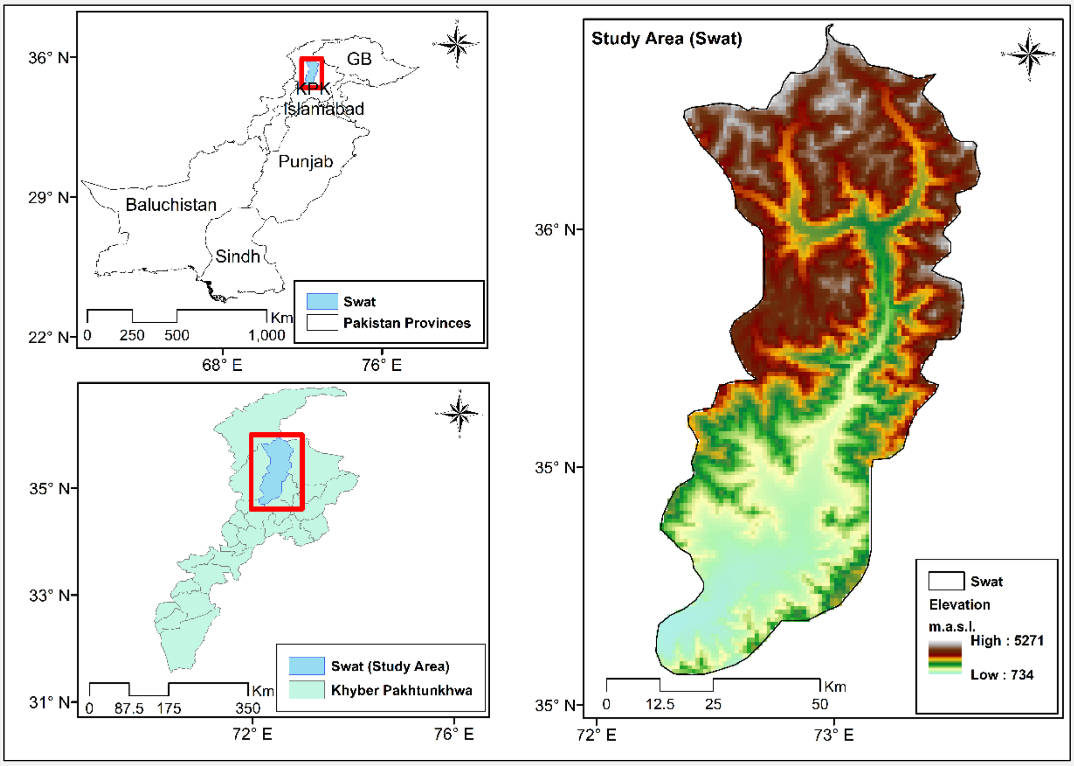

Figure 1. Study Area Map for Swat, Khyber Pakhtunkhwa Pakistan.

In 2012, heavy monsoon rains caused floods in major parts of Pakistan, including Khyber Pakhtunkhwa, Upper Sindh, Southern Punjab, and Baluchistan provinces (Saeed et al., 2021; Shah et al., 2023). In August 2013, the country experienced catastrophic flash flood following devastating flood events (Butt et al., 2020), causing 1,486 deaths, including 530 children (NDMA, 2022). In the recent monsoon floods of 28 August 2022 "the monster flood" severely impacted one third of the country (Otto et al., 2022), Pakistan suffered 1,486 deaths including 530 children, 32 million people were affected, over 450,000 residential structures were damaged, 149 bridges were destroyed, and 110 districts were affected (NDMA, 2022; PMD, 2022), the flood caused an economic loss of over 30 billion (Otto et al., 2022) The flood caused direct impacts, led to famine due to agricultural devastation, and potentially caused disease outbreaks in temporary shelters (Baqir et al., 2012). Pakistan has experienced six major floods in the last 12 years, disproportionately affecting one-third of the world's fifth-largest populous country, highlighting its vulnerability to climate extremes (Ahmed et al., 2023; Majeed et al., 2023).

The Swat River Basin is facing frequent and intense floods due to climatic variations and diverse topography. The region has experienced catastrophic flood events, such as the 2010 and 2022 floods. However, there is limited research on flood inundation assessment and mapping, highlighting the urgent need for advanced techniques for flood inundation mapping in the Swat. Flood hazard assessment and mapping are crucial for protecting infrastructure and human lives. They focus on flood hazard (inundation depth and extent) and exposure (land use/landcover). Management of flood hazard is shifting from a structure-based approach to a non-structure approach, evaluating mitigation measures' impact on downstream communities (de Kok & Grossmann, 2010; Ernst et al., 2010; Yi et al., 2010). This study uses 10 m resolution Sentinel-2 Imagery supervised classification to identify decreased built-up, land cover, and increased water area impacted by floods. The spectral indices show the severity of the flood downstream, indicating the need for swift mitigation measures to reduce future losses.

Flood-Prone characteristics

June is the hottest month with mean temperatures of 33°C and 16°C, while January is the coldest. The Swat River, a perennial river fed by rain, snow, and glaciers, experienced severe flooding in 2022. The Swat division is a significant flood-prone basin in Pakistan (Ahmed et al., 2023; Nasir et al., 2020). The region's risk of flooding is exacerbated by its diverse climatic conditions, complex topography, and fragile socioeconomic conditions (Mahmood & Jia, 2019). Despite the frequent and intense flooding in Swat, no suitable measures have been taken to hinder or reduce losses from flood hazards.

MATERIALS & METHODS

Remote Sensing (RS) and Geographic Information Systems (GIS) have enhanced man's capability to look at the world with sensors to observe the dynamic changes on the Earth's surface. This revolution has made it quite easy for the human beings to determine changes spatially as well as temporally over a larger area. Among the various application in geoscience and natural resources management, the environmental and climatological aspects are particularly well understood by RS and GIS (Alam et al., 2018; Kannaujiya et al., 2021; Taloor et al., 2020). This study focuses on the Swat division, utilizing Google Earth Engine (GEE) to process satellite imagery and precipitation data for flood assessment and LULC classification. The objectives are to map the LULC changes, assess flood mapping and analyze long-term precipitation trends.

Sentinel-2 images were used for supervised classification in 2021 and 2022. The sentinel-2 MSI operates at a 10-m resolution, suitable for high-resolution LULC and flood assessments. The LULC classes were generated using GEE, and accuracy assessment was applied. The classification process utilized algorithms and spectral homogeneity to categorize land cover into seven classes (Table 1). Supervised classification, which is semi-automatic and more accurate than unsupervised classification, requires prior knowledge of the classes for a sufficient number of pixels to be recognized by the analyzer or a field search. Classification patterns are shown in Table 1. And the specification for the imagery and platform used are shown in Table 2.

Table 1. Classification pattern for LULC

LULC types	Description
Bare land	Open land, sand fillings, unused or empty areas
Built-up	Roads, residential and commercial places
Crops	Agricultural land
Grassland	Rangelands and parks area
Snow/Glaciers	Snowy and glacierized regions
Trees	Mixed Forest, Dense trees
Water	River, lakes, swamps ponds, streams and canals etc.

Table 2. Specification of Imagery used

Mission	Date	Information	Platform	Resolution
Sentinel-2 MSI	July 2021	Before Flood	GEE	10 m
Sentinel-2 MSI	August- 2022	After Flood	GEE	10 m

Flood Assessment

Flood assessment followed the method used by Xue et al. (2022), the methodology involves analyzing SPWB and NDFI to extract flood information. Post-flood changes are established by analyzing the chosen area through terrain reflectivity and vegetation indices. Three indices, NDFI, normalized difference vegetation index (NDVI), and modified normalized difference water index (mNDWI), were extracted from Sentinel-2 (10m resolution) for analysis. The methodology, which is based on the NDFI and SPWB framework, attempts to visually analyze flood maps in order to identify any misclassifications or omissions. The suggested framework finds the flooded locations and uses NDFI to extract the damages produced in the flood-prone zone. The likelihood of a water area is found by combining a number of remote sensing indices, and the SPWB exclusion layer is used to optimize the first extracted findings in order to determine the range of permanent water bodies.

The Sentinel-2 dataset is preprocessed for the study area, and the flood index is calculated using NDFI, a multi-time statistical analysis of two sets of SAR images, with one set containing non-flood period images (Jones et al., 2009), whereas the method calculates the average and minimum backscatter values of each pixel in reference and flood images, then uses two statistical data to derive and generate NDFI, the standardized difference between the mean (reference) and the minimum (reference + flood), by comparing the two images separately. The calculation formula is as follow:

$$NDFI = \frac{mean\sigma 0 \text{ (reference)} - min\sigma 0 \text{ ("}reference + flood\text{")}}{mean\sigma 0 \text{ (reference)} + min\sigma 0 \text{ ("}reference + flood\text{")}} \quad \text{(Jones et al., 2009)} \quad (1)$$

Among them, mean ("reference") represents the average backscatter coefficient of pixel of the reference image, and min ("reference + flood") refers to the minimum value of the image each pixel backscatter coefficient.

When calculating NDFI, the mean and min values of some picture elements are different, causing the NDFI to be much greater than 0 or less than −1. This result will affect the calculation of the NDFI threshold, and in turn affects the accuracy of the experimental results. Therefore, outliers, such as a picture element that is smaller than −1 or larger than 0, should be removed. After removing the outliers, the appropriate threshold for flood extraction could be determined more accurately. The threshold calculation formula is as follows:

$$th = mean\ (NDFIflood) - k \times std\ (NDFIflood) \quad \text{(Cian et al., 2018)} \quad (2)$$

Among them, *th* represents the threshold, mean (NDFIflood) represents the average value of the entire difference image, and std (NDFIflood) stands for the standard deviation of the entire difference image. After the abnormal value is removed, a constant threshold is used to segment flood areas. Having conducted several case studies, (Cian et al., 2018) verified that k = 1.5 is the most effective value. The areas less than the threshold are flooded areas.

The modified normalized difference water index (mNDWI) is one of the most widely used and the most effective methods to distinguish the characteristics of water body areas by using the normalized difference between the green band and the short-wave infrared band of remote sensing images (Verpoorter et al., 2012). However, owing to the mixed distribution of aquatic plants in wetlands, mNDWI still has errors in distinguishing water bodies from vegetation (Xu, 2006). Many studies showed that the combination of mNDWI, NDVI (Xu et al., 2021), and enhanced vegetation index (EVI) is much better and more stable than a single index in the mapping of flood. The criteria of EVI below 0.1 can reduce the interference of wetland vegetation on wetland water extraction. We use the combination of mNDWI, NDVI, and EVI to extract water areas and combine the two standards of mNDWI > NDVI and EVI < 0.1, or mNDWI > EVI and EVI < 0.1 to identify surface water.

The Normalized Difference Vegetation Index (NDVI) is an indicator that uses the red and near-infrared spectral bands. It is one of the most well-known used vegetation indices and highly associated with vegetation content (Rouse et al., 1973; USGS, 2019).

$$NDVI = \frac{(NIR - RED)}{(NIR + RED)} \quad \text{(Rouse et al., 1973; USGS, 2019)} \quad (3)$$

Modified Normalized Difference Water Index (mNDWI) is used for water bodies analysis, can enhance open water features while efficiently suppressing and even removing built-up land noise as well as vegetation and soil noise. The mNDWI is more suitable for enhancing and extracting water information for a water region with a background dominated by built-up land areas because of its advantage in reducing and even removing built-up land noise over the NDWI (Xu, 2006).

$$mNDWI = \frac{(Green - SWIR)}{(Green + SWIR)} \quad \text{(Rouse et al., 1973; USGS, 2019)} \quad (4)$$

Enhanced Vegetation Index (EVI) is similar to the Normalized Difference Vegetation Index (NDVI) and can be used to quantify vegetation greenness. However, EVI corrects for some atmospheric conditions and canopy background noise and is more sensitive in areas with dense vegetation (Cheng & Liang, 2018; Gao, 1996).

$$EVI = \frac{2.5 \times ((NIR - RED)}{(NIR + 6 \times RED - 7.5 \times BLUE + 1))} \quad \text{(Cheng \& Liang, 2018; Gao, 1996)} \quad (5)$$

Given the applicability of NDFI in rivers and lakes needs to be improved, we used a framework by combining NDFI calculated from SAR images and SPWB exclusion layer as NDFI-SPWB. The criteria for calculating the indices for the SPWB layer is to get the EVI < 0.1, and then combine with the mNDWI, NDVI and the water areas were then extracted also shown in the flow chart Figure 2. This framework can give full play advantage to the characteristics of the exclusion layer and retain the advantages of NDFI. It can also quickly and accurately conduct large scale flood monitoring. The framework is mainly based on the SAR data using the NDFI to initially extract flood damage in the study area and obtain the flood inundation area.

Accuracy Assessment

The accuracy assessment of various image processing procedures in image classification was evaluated for different LULC classifications in Swat division between 2021 and 2022, highlighting its importance in image classification.

$$Overall\ accuracy = \frac{Number\ of\ sampling\ classes\ classified\ correctly}{Number\ of\ reference\ sampling\ classes} \quad \text{(Monserud \& Leemans, 1992)} \ (6)$$

The kappa coefficient values are estimate of how well remote sensing classification is correct and agree with reference data. Conceptually Kappa is defined as:

$$kappa\ Coefficient = \frac{observed\ acciracy - chance\ agreement}{1 - chance\ agreement} \quad \text{(Monserud \& Leemans, 1992)} \ (7)$$

The study's average accuracy kappa coefficient was 98.55% and 98.26% for 2021 and 2022, indicating significant compatibility with ground observation of land cover classes. A kappa coefficient of 70% or greater signifies ‘very good' compatibility (Monserud & Leemans, 1992). . The LULC classification showed significant alignment with ground observation, indicating a high level of compatibility with land cover classifications.

Climate Data

Daily Climate Hazards Group Infrared Precipitation with Station data (CHIRPS) data from 1989 to 2022 was processed in GEE for the Swat division, integrating satellite-based global data with in-situ station data to create a synthetic gridded rainfall time series (Funk et al., 2015). The analysis of data for only the summer months i.e., June, July, August and September (JJAS), from 1989 to 2022 compares significant changes in 2022 and the past in the spatial extent of Swat division. CHIRPS data has a coarser resolution of 0.05 degrees, appropriate for regional climate analysis. Figure 2 contains the detailed methodology flow chart for this study.

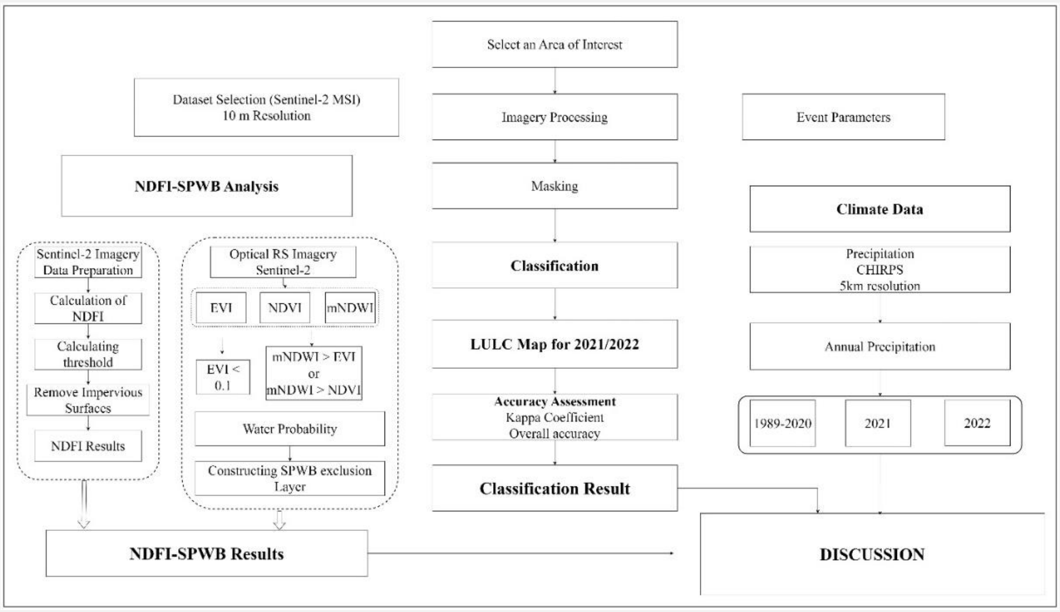

Figure 2. Methodology flow chart.

RESULTS

The study of land use and land cover change (LULC) as a metric for monitoring and controlling global ecological changes has been recently utilized. The study uses GEE to analyze LULC changes in Swat, Pakistan, identifying seven classes: bare land, built-up, crops, grassland, snow/ice, trees, and water bodies. Figure 3 displays different LULC classes for 2021 and 2022.

LULC Changes

In 2022, a total of 60 km² of forest was reduced which makes -6.8 of its loss%, 16% of cropland was impacted, over 8% of built-up/property was damaged, 13% of bare land was increased, and 50 km² of water bodies were inundated, resulting in a total of 258 km² of land use change during one year. The classified land use land cover map is show in the Figure 3 for the year 2021 and 2022. With the change statistics is plotted in the Figure 4 with statistics. Figure 5 shows the land use change results during one year between 2021 and 2022.

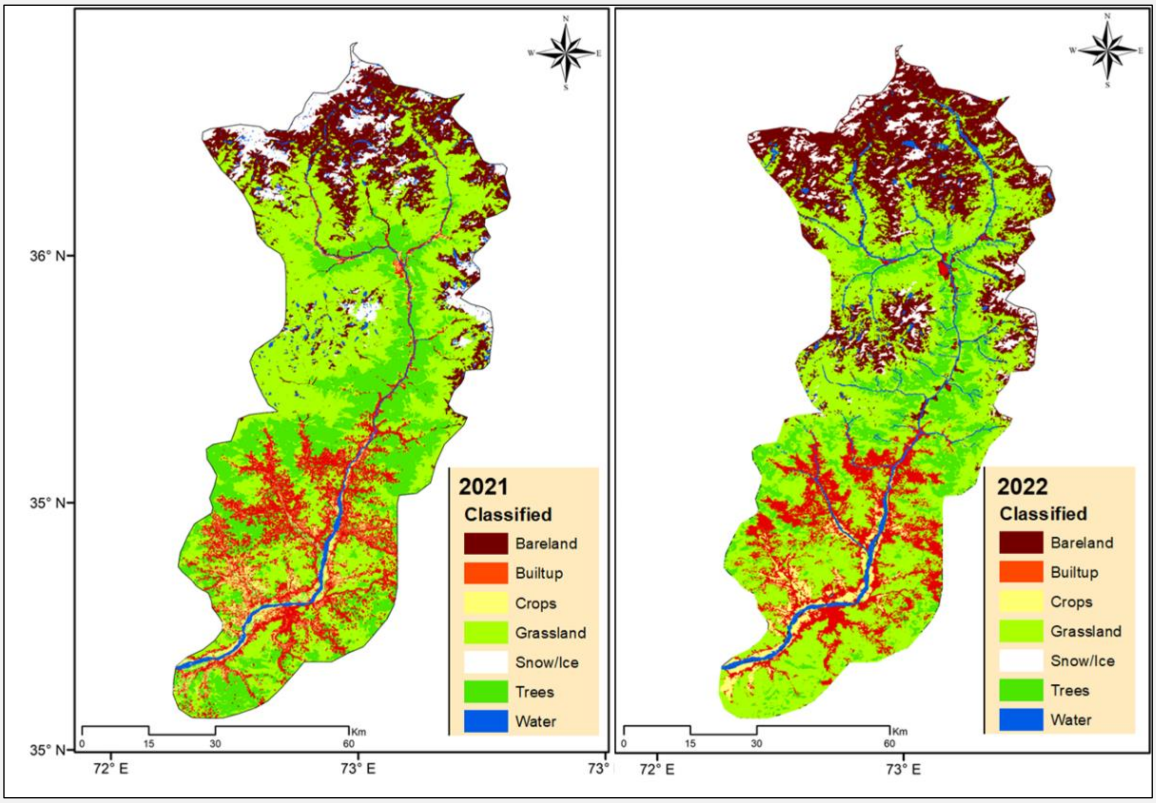

Figure 3. Supervised Classification for the year 2021 and 2022.

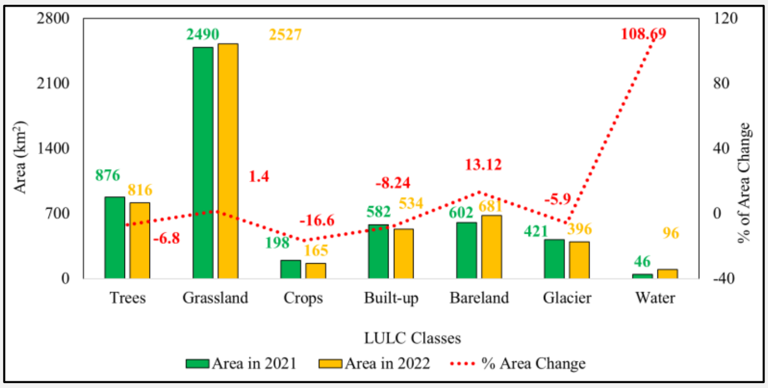

Figure 4. Rate of LULC changes between 2021 and 2022.

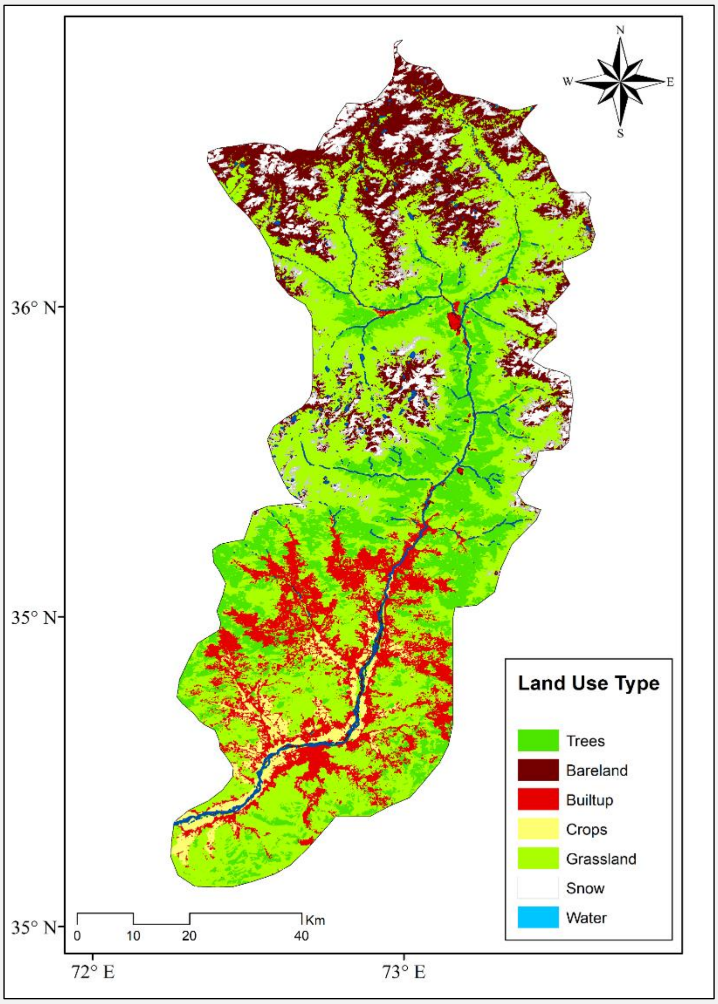

Figure 5. Land Use Change during 2021 and 2022 for Swat division.

Flood Inundation

The Sentinel-2 Images are preprocessed to determine the spatial distribution of flood effected areas, with the exception of water permanent water bodies or summer permanent water bodies. The NDFI-SPWB framework calculates flood damage distribution maps in the Swat division, with red indicating flood inundated areas and 1230 km^2 calculated flood areas. Figure 6 is the spatial distribution of the SPWB-NDFI for the Swat region.

Precipitation Analysis

Global warming has intensified extreme weather events, including precipitation, posing significant threats to the environment, society, and human health. Annual precipitation data for Swat division was processed through CHIRPS from 1989 to 2022. From 1989 to 2021, the Swat region experienced the summer average precipitation of 131-764 mm while highest in the northern parts and southern and central Swat. However, in 2022, during a massive flood, the summer precipitation the highest rainfall received increased to 877 mm, with the Central, southern and northern parts received precipitation more than 500 mm during 2022 and with the causing extreme levels of precipitation in both the north and south as shown in the Figure 7.

The flood in Mingora Swat, Madian Swat, and its surrounding areas in 2021 and 2022 significantly impacted the surrounding areas and roads, as evidenced by the increased water levels in the river swat and surrounding areas (Figure 7). The Madian River and Mingora in Swat are a striking tribute to the force of change in the visual representation of nature's transformation. Snaps of the satellite imagery for the years 2021 and 2022 from Sentinel-2, clearly portray the impact of a key event. The record of recent history, the year 2022 was significant as the region witnessed a terrible flood. Images from this year show rivers pushed beyond their breaking points; banks shattered by the unrelenting onslaught of water. An enduring symbol of nature's breathtaking strength, shifting landscapes, and prompting contemplation on the complex relationship between our environment and the forces that shape it.

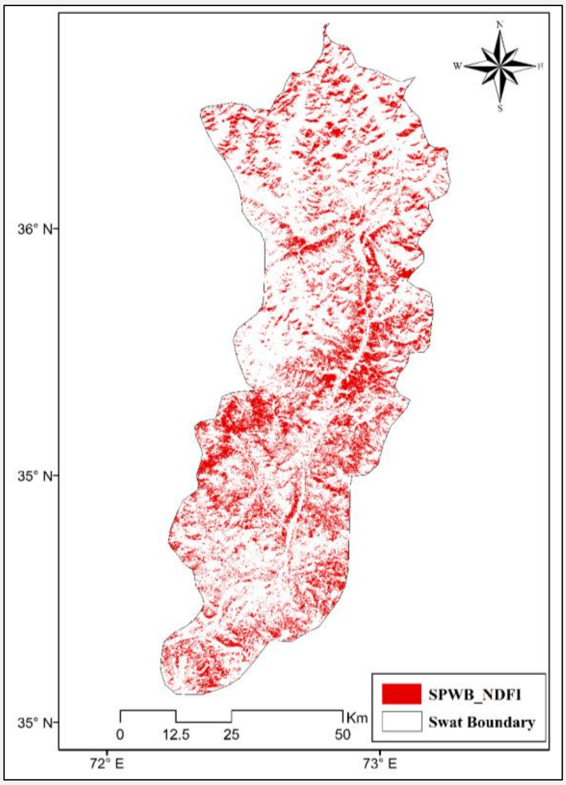

Figure 6. SPWB-NDFI results of Swat.

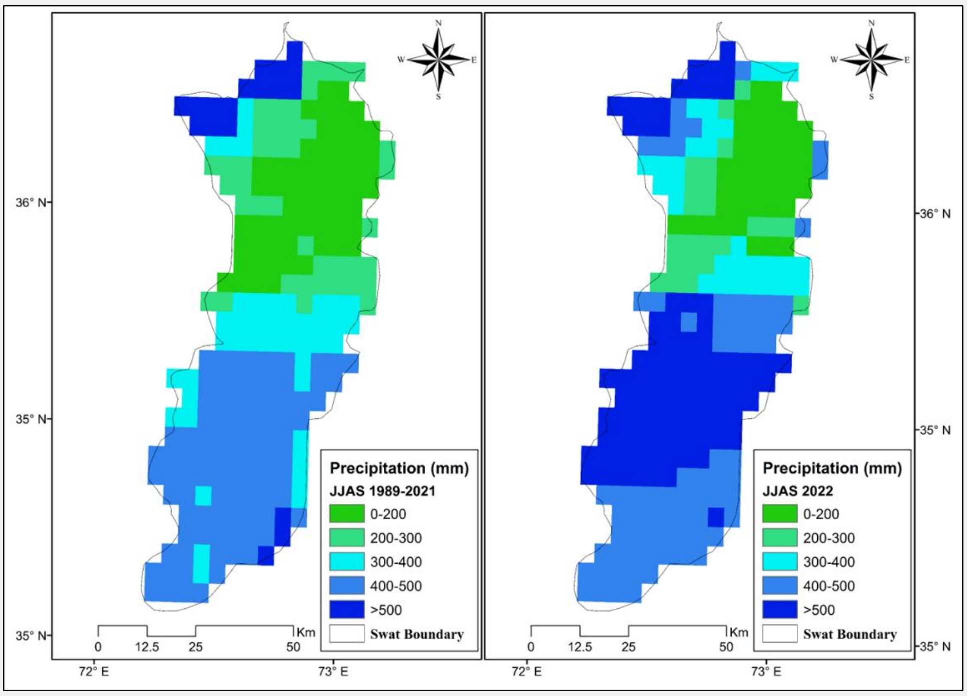

Figure 7. Summer Precipitation from 1989 to 2022 and the summer precipitation for the year 2022.

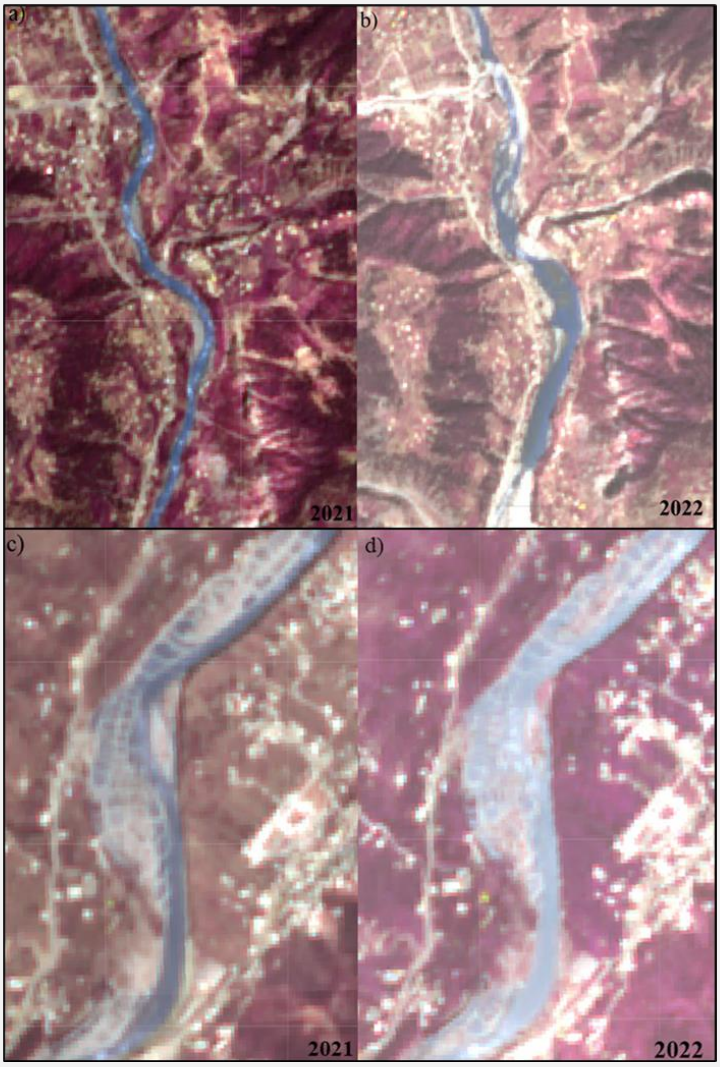

Figure 8. Snaps of river Swat from Madian swat (a and b), and Mingora (c and d) for 2021 and 2022.

DISCUSSION

The findings of this study highlight the effectiveness of integrating the Normalized Difference Flood Index (NDFI) with the Summer Permanent Water Bodies (SPWB) exclusion layer in accurately mapping flood inundation areas in the Swat region. By utilizing Sentinel-2 satellite imagery and Synthetic Aperture Radar (SAR) data, the methodology enabled a robust delineation of flood-affected zones during the 2022 monsoon season, a year marked by one of the most severe flood events in recent history. These results align with earlier studies that have demonstrated the utility of remote sensing techniques in large-scale flood monitoring (Jones et al., 2009; Xue et al., 2022), further reinforcing their applicability in complex topographies such as the Hindukush region.

Flood Impacts and Mitigation strategies in Pakistan

Floods are among the most destructive natural disasters globally, causing extensive damage to livelihood, economics, agriculture, environment and property. Pakistan, particularly the Swat region in Khyber Pakhtunkhwa, experiences the severe impacts caused by climate change induced precipitation variations. The exception monsoon triggering the 2022 flood highlighting critical needs for advanced mapping and assessment like GIS and RS to mitigate damages. This study finds the application in assessing the flood, focusing on the novel NDFI-SPWB framework, land cover changes and implications for flood management. Mitigating these effects, especially in developing countries, is challenging. Authorities and policymakers face difficulties in protecting lives and minimizing economic and environmental losses (Akbar et al., 2024). There is a pressing need for accurate and timely information about flash floods, as well as the development and implementation of effective strategies.

Effective Remote Sensing Methodology

The present study assessed the 2022 flood in Swat division Pakistan using GIS and RS techniques, analyzing data on satellite image classification, NDFI-SPWB (primarily based on the EVI, NDVI and mNDWI), and CHIRPS precipitation. in determining the danger of flooding in Swat, Khyber Pakhtunkhwa Pakistan. The NDFI method is efficient but misclassifies some permanent water bodies into floods. A new framework, NDFI-SPWB, combines NDFI from SAR images with SPWB exclusion layer., which is better and outstanding performances in the lake and river areas.

The NDFI-SPWB framework improves user accuracy by about 10% and Kappa coefficient by about 0.08 compared to the original NDFI method, verified by flood event in the Yangtze river basin in July 2020, confirming its feasibility and effectiveness, and this method improves the accuracy and also reduces the errors that are caused by the characteristics of NDFI methods, which sometimes includes the permanent water bodies as the flooded areas (Xue et al., 2022).

The application of the NDFI method, derived from multi-temporal SAR images, allowed for the differentiation between permanent water bodies and temporary floodwater surfaces. The index was calculated using the formula:

$$NDFI = \frac{mean\sigma 0 \text{ (reference)} - min\sigma 0 \text{ ("}reference + flood\text{")}}{mean\sigma 0 \text{ (reference)} + min\sigma 0 \text{ ("}reference + flood\text{")}} \tag{8}$$

This approach proved effective in identifying flooded areas even under cloud cover, which often hampers optical satellite observations. The integration of the SPWB exclusion layer further refined the flood maps by eliminating confusion between seasonal water bodies and actual inundation zones. As a result, the classification achieved an overall accuracy of 98% and a kappa coefficient of 97.5%, demonstrating high reliability and consistency in image interpretation.

These results are consistent with global applications of similar methodologies (Xue et al., 2022), where NDFI-based flood detection has shown strong performance in both rural and urban landscapes. However, this study adds regional specificity by applying these tools in a mountainous, data-scarce environment, thereby expanding the evidence base for flood monitoring in South Asia.

Comparative studies, such as Khan et al. (2025) in Swat, used the Analytic Hierarchy Process (AHP) with GIS, focusing on parameters like elevation, slope, and rainfall, while Rahman et al., (2023) applied a bivariate statistical model for flood susceptibility mapping in the Swat River Basin. These studies highlight the diversity of approaches, with NDFI-SPWB offering a more direct, imagery-based solution for real-time flood mapping, particularly effective in distinguishing temporary flood waters from permanent water bodies.

Land Cover Change and Economic Implications

The study found that the area covered by trees decreased by over 6% between 2021 and 2022, while built-up areas were impacted by over 8% (Table 3). The built-up area was impacted by 13%, while baren land increased by 13%. The crop lands are impacted by about 16% and it is considered the main land cover class at risk and exposure as is directly linked with the economy generation for the province (Ahmed et al., 2024). The overall accuracy was 99.7% for 2021 and 97.3% for 2022. Vegetation indices and classification are the most accurate methods, as they were quick and easy to calculate (Xue et al., 2022; Huang et al., 2021).

Table 3. Highlighted the change in the main LULC classes

Land Cover Type	Change (2021-2022)	Percentage Impacts
Tree Cover	Decreased	~6%
Built-up	Increased	~8%
Barren land	Increased	~13%
Croplands	Increased	~16%

These changes reflect the broader trend of flood-induced land cover alterations, with agricultural areas being the most exposed, directly linked to economic generation for the province (Ahmed et al., 2024). The 2022 floods significantly altered land use patterns in the Swat region, particularly around riverbanks and agricultural plains. Post-flood analysis using Google Earth Engine and the Random Forest algorithm revealed extensive erosion, sediment deposition, and loss of arable land. These changes underscore the vulnerability of local communities to recurrent flooding, especially those residing in low-lying or poorly planned settlements.

Such disruptions not only threaten livelihoods but also exacerbate existing socio-economic inequalities, particularly among subsistence farmers and marginalized groups. This aligns with broader findings from political ecology literature, which emphasizes how environmental hazards disproportionately affect vulnerable populations due to unequal access to resources and decision-making power (Zhou et al., 2024). In this context, flood-induced displacement and land degradation may reinforce cycles of poverty and food insecurity.

Precise Delineation of Climate-Driven Flood Inundation in Swat Using SPWB-NDFI

This study uses precipitation and satellite imagery to extract flood-inundated areas and processed satellite images for supervised classification in 2021 and 2022. It combines SPWB-NDFI information and classification to estimate flood inundation, highlighting common causes in areas with heavy rainfall exceeding capacity, it is robust and advanced flood mapping, by excluding the summer permanent water bodies, the results are more accurate and only the flood inundated areas due to the catastrophe are mapped through this interesting method.

Induced precipitation variations due to climate change poses grave environmental, infrastructure, and health risks, intensely in populated regions (Shen et al., 2022; Wattanachareekul et al., 2023). In 2022, highest summer precipitation falls in Swat, causing extreme levels of flood in the region. The research focused on flood inundation mapping of swat region for 2022, employing a novel technique, with utilizing the LULC for the region before and after the flood. RS and GIS provides consistent information for effective flood management and monitoring in Pakistan (Uddin et al., 2013).

Accuracy and Validation

The study's classification methods achieved high overall accuracy, with 99.7% for 2021 and 97.3% for 2022, leveraging vegetation indices like EVI and NDVI, which are noted for their quick and easy calculation (Xue et al., 2022; Huang et al., 2021). The NDFI-SPWB framework's robustness was further validated by excluding summer permanent water bodies, ensuring that only flood-inundated areas due to the catastrophe were mapped, enhancing accuracy for disaster response.

Policy Implications and Disaster Risk Reduction

The increasing frequency and intensity of extreme weather events linked to climate change (Abbas et al., 2023). Therefore, there is an urgent need for improved flood risk management strategies in Pakistan. Our findings suggest that remote sensing-based flood mapping can serve as a valuable tool for early warning systems, emergency response planning, and long-term adaptation policies.

One key policy implication is the integration of satellite-derived flood maps into local governance frameworks. For instance, spatially explicit data can inform zoning regulations, infrastructure development, and ecosystem-based adaptation measures such as wetland restoration and riparian buffer zones that reduce exposure to flood risks. Moreover, participatory approaches involving local stakeholders should be prioritized to ensure that flood mitigation strategies are contextually appropriate and socially inclusive. Drawing from conservation and community forestry models (Hajjar et al., 2021), collaborative floodplain management could empower communities to co-develop resilience strategies, combining scientific knowledge with indigenous practices.

The significance of this study lies in its applied implications. The flood map produced by our study serve as valuable tools for urban planners, local authorities, and disaster management agencies. By applying these results, stakeholders can proactively promote sustainable development and enhance regional resilience to minimize flood hazard impacts. This application is particularly vital in developing countries like Pakistan, where challenges in protecting lives and minimizing economic and environmental losses are significant (Uddin et al., 2013). Furthermore, the study's focus on precipitation variations due to climate change aligns with global research, emphasizing the consistent need for RS and GIS information for effective flood management and monitoring.

CONCLUSION

This study uses remote sensing, geospatial data, and climatic statistics to examine the connection between flood inundation and annual precipitation patterns. Google Earth Engine's Supervised Classification for Sentinel-2 Imagery was utilized, achieving an accuracy rate of 99.7% for 2021 and

97.3% for 2022. Flood water body levels are scrutinized, leads to an illuminating flood inundation map. The total land use change area in 2022 reached 258 km^2, with a total inundation area spanning 1230 km^2. The analysis of Climate Hazards Group InfraRed Precipitation with Station (CHIRPS) summer data reveals a severe increase in the southern, central, and northern parts of Swat in 2022. This study aims to advance flood mapping understanding and offer a roadmap for enhanced disaster management strategies in the Swat region and beyond. The findings of this study provide critical insights for urban planners, local authorities, and disaster management agencies in flood-prone regions such as Swat. The detailed flood inundation maps generated through this research facilitate informed decision-making regarding land use planning, emergency response protocols, and the implementation of targeted flood mitigation measures. To enhance resilience, it is recommended by the National Disaster Risk Management and the Pakistan Meteorological Department to increase public awareness of flood risks, identify and designate safe areas for evacuation, and to avoid practices that obstruct river flows or impede natural drainage systems, such as unauthorized dam construction for irrigation. Additionally, guidelines for siting residential and commercial structures at safe distances from riverbanks and high-risk zones should be developed and strictly adhered to, in order to minimize the potential impact of flooding on lives and infrastructure.

Software

Data analysis was performed using cloud computing platforms Google Earth Engine and all maps were created using ArcGIS 10.8.

Acknowledgments

The authors gratefully acknowledge the use of satellite imagery and climate data from the following open-source platforms and institutions: European Space Agency (ESA) for providing Sentinel-2 satellite imagery through the Copernicus Open Access Hub (https://scihub.copernicus.eu/); Google Earth Engine (GEE) platform for facilitating large-scale geospatial analysis and access to multi-temporal datasets; Climate Hazards Group InfraRed Precipitation with Station data (CHIRPS) for providing high-resolution precipitation data, available at https://chirps.geog.ucsb.edu/; United States Geological Survey (USGS) and NASA for supporting remote sensing research and data accessibility. We also thank the journal reviewers and editors for their insightful comments and suggestions that helped improve the quality of this manuscript.

Disclosure Statement

The authors have no potential conflict of interest.

Data availability Statement

The data in this study area available from the first and corresponding authors upon reasonable request.

Conflict of Interest

There is no conflict of interest.

REFERENCES

Abbas, A., Bhatti, A. S., Ullah, S., Ullah, W., Waseem, M., Zhao, C., Dou, X., & Ali, G. (2023). Projection of precipitation extremes over South Asia from CMIP6 GCMs. *Journal of Arid Land*, *15*(3), 274-296. https://doi.org/10.1007/s40333-023-0050-3

Abbas, A., Ullah, S., Ullah, W., Waseem, M., Dou, X., Zhao, C., Karim, A., Zhu, J., Hagan, D. F. T., Bhatti, A. S., & Ali, G. (2022). Evaluation and projection of precipitation in Pakistan using the Coupled Model Intercomparison Project Phase 6 model simulations. *International Journal of Climatology*, *42*(13), 6665-6684. https://doi.org/https://doi.org/10.1002/joc.7602

Ahmed, E., Saddique, N., Al Janabi, F., Barfus, K., Asghar, M. R., Sarwar, A., & Krebs, P. (2023). Flood Predictability of One-Way and Two-Way WRF Nesting Coupled Hydrometeorological Flow Simulations in a Transboundary Chenab River Basin, Pakistan. *Remote Sensing*, *15*(2), 457. https://www.mdpi.com/2072-4292/15/2/457

Akbar, S., Junbo, W., Atta, U., Yasir, L., & and Muhammad, S. (2024). The growth and emergence of potentially dangerous glacier lakes in Astore Basin, Western Himalaya during 1993–2021. *Geomatics, Natural Hazards and Risk*, *15*(1), 2353838. https://doi.org/10.1080/19475705.2024.2353838

Alam, A., Bhat, M. S., Kotlia, B. S., Ahmad, B., Ahmad, S., Taloor, A. K., & Ahmad, H. F. (2018). Hybrid tectonic character of the Kashmir basin: response to comment on "Coexistent pre-existing extensional and subsequent compressional tectonic deformation in the Kashmir basin, NW Himalaya (Alam et al., 2017)" by Shah (2017). *Quaternary International*, *468*, 284-289.

Almazroui, M., Saeed, S., Saeed, F., Islam, M. N., & Ismail, M. (2020). Projections of Precipitation and Temperature over the South Asian Countries in CMIP6. *Earth Systems and Environment*, *4*(2), 297-320. https://doi.org/10.1007/s41748-020-00157-7

Atta ur, R., & Khan, A. N. (2013). Analysis of 2010-flood causes, nature and magnitude in the Khyber Pakhtunkhwa, Pakistan. *Natural Hazards*, *66*(2), 887-904. https://doi.org/10.1007/s11069-012-0528-3

Baqa, M. F., Lu, L., Chen, F., Nawaz-ul-Huda, S., Pan, L., Tariq, A., Qureshi, S., Li, B., & Li, Q. (2022). Characterizing Spatiotemporal Variations in the Urban Thermal Environment Related to Land Cover Changes in Karachi, Pakistan, from 2000 to 2020. *Remote Sensing*, *14*(9), 2164. https://www.mdpi.com/2072-4292/14/9/2164

Baqir, M., Sobani, Z. A., Bhamani, A., Bham, N. S., Abid, S., Farook, J., & Beg, M. A. (2012). Infectious diseases in the aftermath of monsoon flooding in Pakistan. *Asian Pacific Journal of Tropical Biomedicine*, *2*(1), 76-79. https://doi.org/https://doi.org/10.1016/S2221-1691(11)60194-9

Bhatti, A. S., Wang, G., Ullah, W., Ullah, S., Fiifi Tawia Hagan, D., Kwesi Nooni, I., Lou, D., & Ullah, I. (2020). Trend in Extreme Precipitation Indices Based on Long Term In Situ Precipitation Records over Pakistan. *Water*, *12*(3), 797. https://www.mdpi.com/2073-4441/12/3/797

Billa, L., Shattri, M., Rodzi Mahmud, A., & Halim Ghazali, A. (2006). Comprehensive planning and the role of SDSS in flood disaster management in Malaysia. *Disaster Prevention and Management: An International Journal*, *15*(2), 233-240. https://doi.org/10.1108/09653560610659775

Butt, A., Aslam, H. M. U., Shabir, H., Javed, M., Hussain, S., Nadeem, S., Raza, H., Haroon, S., & Arshad, S. (2020). Climatic Events and Natural Disasters of 21st Century: A Perspective of Pakistan.

Chen, Y., Opała-Owczarek, M., Chen, F., Owczarek, P., Zhang, H., Wang, S., Hu, M., Satylkanov, R., Ermenbaev, B., Zulfiyor, B., Shang, H., & Zhang, R. (2023). Tree-ring perspective on past and future mass balance of the glaciers in Tien Shan (Central Asia): An example from the accumulation area of Tuyuksu Glacier, Kazakhstan. *Palaeogeography, Palaeoclimatology, Palaeoecology*, *625*, 111696. https://doi.org/https://doi.org/10.1016/j.palaeo.2023.111696

Cheng, J., & Liang, S. (2018). 5.10 - Land-Surface Emissivity. In S. Liang (Ed.), *Comprehensive Remote Sensing* (pp. 217-263). Elsevier. https://doi.org/https://doi.org/10.1016/B978-0-12-409548-9.10374-4

Cian, F., Marconcini, M., & Ceccato, P. (2018). Normalized Difference Flood Index for rapid flood mapping: Taking advantage of EO big data. *Remote sensing of environment*, *209*, 712-730. https://doi.org/https://doi.org/10.1016/j.rse.2018.03.006

de Kok, J.-L., & Grossmann, M. (2010). Large-scale assessment of flood risk and the effects of mitigation measures along the Elbe River. *Natural Hazards*, *52*(1), 143-166. https://doi.org/10.1007/s11069-009-9363-6

Dereli, T., Eligüzel, N., & Çetinkaya, C. (2021). Content analyses of the international federation of red cross and red crescent societies (ifrc) based on machine learning techniques through twitter. *Natural Hazards*, *106*, 2025-2045.

Díez-Herrero, A., & Garrote, J. (2020). Flood risk analysis and assessment, applications and uncertainties: A bibliometric review. *Water*, *12*(7), 2050.

Ernst, J., Dewals, B. J., Detrembleur, S., Archambeau, P., Erpicum, S., & Pirotton, M. (2010). Micro-scale flood risk analysis based on detailed 2D hydraulic modelling and high resolution geographic data. *Natural Hazards*, *55*(2), 181-209. https://doi.org/10.1007/s11069-010-9520-y

Farooq, M., Shafique, M., & Khattak, M. S. (2019). Flood hazard assessment and mapping of River Swat using HEC-RAS 2D model and high-resolution 12-m TanDEM-X DEM (WorldDEM). *Natural Hazards*, *97*(2), 477-492. https://doi.org/10.1007/s11069-019-03638-9

Funk, C., Peterson, P., Landsfeld, M., Pedreros, D., Verdin, J., Shukla, S., Husak, G., Rowland, J., Harrison, L., Hoell, A., & Michaelsen, J. (2015). The climate hazards infrared precipitation with stations—a new environmental record for monitoring extremes. *Scientific Data*, *2*(1), 150066. https://doi.org/10.1038/sdata.2015.66

Gao, B.-c. (1996). NDWI—A normalized difference water index for remote sensing of vegetation liquid water from space. *Remote sensing of environment*, *58*(3), 257-266. https://doi.org/https://doi.org/10.1016/S0034-4257(96)00067-3

Gaurav, K., Sinha, R., & Panda, P. K. (2011). The Indus flood of 2010 in Pakistan: a perspective analysis using remote sensing data. *Natural Hazards*, *59*(3), 1815-1826. https://doi.org/10.1007/s11069-011-9869-6

Hajjar, R., Oldekop, J. A., Cronkleton, P., Newton, P., Russell, A. J., & Zhou, W. (2021). A global analysis of the social and environmental outcomes of community forests. *Nature sustainability*, *4*(3), 216-224. https://doi.org/10.1038/s41893-020-00633-y

Huang, Y., Shi, W., Fu, Q., Qiu, Y., Zhao, J., Li, J., Lyu, Q., Yang, X., Xiong, J., Wang, W., Chang, R., Yao, Z., Dai, Z., Qiu, Y., & Chen, H. (2023). Soil development following glacier retreat shapes metagenomic and metabolomic functioning associated with asynchronous C and N accumulation. *Science of the Total Environment*, *892*, 164405. https://doi.org/https://doi.org/10.1016/j.scitotenv.2023.164405

Jones, K., Lanthier, Y., van der Voet, P., van Valkengoed, E., Taylor, D., & Fernández-Prieto, D. (2009). Monitoring and assessment of wetlands using Earth Observation: The GlobWetland project. *Journal of Environmental Management*, *90*(7), 2154-2169. https://doi.org/https://doi.org/10.1016/j.jenvman.2007.07.037

Kannaujiya, S., Gautam, P. K., Chauhan, P., Roy, P. N. S., Pal, S. K., & Taloor, A. K. (2021). Contribution of seasonal hydrological loading in the variation of seismicity and geodetic deformation in Garhwal region of Northwest Himalaya. *Quaternary International*, *575*, 62-71.
Kawo, N. S., Hordofa, A. T., & Karuppannan, S. (2021). Performance evaluation of GPM-IMERG early and late rainfall estimates over Lake Hawassa catchment, Rift Valley Basin, Ethiopia. *Arabian Journal of Geosciences*, *14*(4), 256.
Khan, N. A., Alzahrani, H., Bai, S., Hussain, M., Tayyab, M., Ullah, S., Ullah, K., & Khalid, S. (2025). Flood risk assessment in the Swat river catchment through GIS-based multi-criteria decision analysis. *Frontiers in Environmental Science*, *13*, 1567796. https://doi.org/10.3389/fenvs.2025.1567796
Khan, A. A., Jamil, A., Hussain, D., Taj, M., Jabeen, G., & Malik, M. K. (2020). Machine-learning algorithms for mapping debris-covered glaciers: The Hunza Basin case study. *Ieee Access*, *8*, 12725-12734.
Khan, I., Ali, A., Waqas, T., Ullah, S., Ullah, S., Shah, A. A., & Imran, S. (2022). Investing in disaster relief and recovery: A reactive approach of disaster management in Pakistan. *International Journal of Disaster Risk Reduction*, *75*, 102975. https://doi.org/https://doi.org/10.1016/j.ijdrr.2022.102975
Khan, I., Lei, H., Shah, A. A., Khan, I., & Muhammad, I. (2021). Climate change impact assessment, flood management, and mitigation strategies in Pakistan for sustainable future. *Environmental Science and Pollution Research*, *28*(23), 29720-29731. https://doi.org/10.1007/s11356-021-12801-4
Lehmann, J., Coumou, D., & Frieler, K. (2015). Increased record-breaking precipitation events under global warming. *Climatic change*, *132*. https://doi.org/10.1007/s10584-015-1466-3
Liu, J., Liu, K., & Wang, M. (2023). A Residual Neural Network Integrated with a Hydrological Model for Global Flood Susceptibility Mapping Based on Remote Sensing Datasets. *Remote Sensing*, *15*(9), 2447. https://www.mdpi.com/2072-4292/15/9/2447
Mahmood, R., & Jia, S. (2019). Assessment of hydro-climatic trends and causes of dramatically declining stream flow to Lake Chad, Africa, using a hydrological approach. *Science of the Total Environment*, *675*, 122-140.
Mahto, S. S., & Mishra, V. (2019). Does ERA-5 Outperform Other Reanalysis Products for Hydrologic Applications in India? *Journal of Geophysical Research: Atmospheres*, *124*(16), 9423-9441. https://doi.org/https://doi.org/10.1029/2019JD031155
Majeed, M., Lu, L., Anwar, M. M., Tariq, A., Qin, S., El-Hefnawy, M. E., El-Sharnouby, M., Li, Q., & Alasmari, A. (2023). Prediction of flash flood susceptibility using integrating analytic hierarchy process (AHP) and frequency ratio (FR) algorithms [Original Research]. *Frontiers in Environmental Science*, *10*. https://doi.org/10.3389/fenvs.2022.1037547
Malik, M. I., & Ahmad, F. (2014). Flood Inundation Mapping and Risk Zoning of the Swat River Pakistan using HEC-RAS Model.
Mirza, M. M. Q. (2011). Climate change, flooding in South Asia and implications. *Regional Environmental Change*, *11*(1), 95-107. https://doi.org/10.1007/s10113-010-0184-7
Monserud, R. A., & Leemans, R. (1992). Comparing global vegetation maps with the Kappa statistic. *Ecological Modelling*, *62*(4), 275-293. https://doi.org/https://doi.org/10.1016/0304-3800(92)90003-W
Nanditha, J. S., Kushwaha, A. P., Singh, R., Malik, I., Solanki, H., Chuphal, D. S., Dangar, S., Mahto, S. S., Vegad, U., & Mishra, V. (2023). The Pakistan Flood of August 2022: Causes and Implications. *Earth's Future*, *11*(3), e2022EF003230. https://doi.org/https://doi.org/10.1029/2022EF003230
Nasir, M. J., Iqbal, J., & Ahmad, W. (2020). Flash flood risk modeling of swat river sub-watershed: a comparative analysis of morphometric ranking approach and El-Shamy approach. *Arabian Journal of Geosciences*, *13*(20), 1082. https://doi.org/10.1007/s12517-020-06064-5
NDMA. (2022). *National disaster management authority, Pakistan.*
Otto, F., Zachariah, M., Saeed, F., Siddiqi, A., Shahzad, K., Mushtaq, H., Achutarao, K., S T, C., Barnes, C., Philip, S., Thalheimer, L., Raju, E., Li, S., Yang, W., Harrington, L., & Clarke, B. (2022). *Final Climate change likely increased extreme monsoon rainfall, flooding highly vulnerable communities in Pakistan.*
Owusu, M., Nursey-Bray, M., & Rudd, D. (2019). Gendered perception and vulnerability to climate change in urban slum communities in Accra, Ghana. *Regional Environmental Change*, *19*. https://doi.org/10.1007/s10113-018-1357-z
Paulikas, M. J., & Rahman, M. K. (2015). A temporal assessment of flooding fatalities in Pakistan (1950–2012). *Journal of Flood Risk Management*, *8*(1), 62-70. https://doi.org/https://doi.org/10.1111/jfr3.12084
PMD. (2022). *Pakistan Meteorological Department.*
Rahman, Z. U., Ullah, W., Bai, S., Ullah, S., Jan, M. A., Khan, M., & Tayyab, M. (2023). GIS-based flood susceptibility mapping using bivariate statistical model in Swat River Basin, Eastern Hindukush region, Pakistan. *Frontiers in Environmental Science*, *11*, 1178540. https://doi.org/10.3389/fenvs.2023.1178540
Rebi, A., Hussain, A., Hussain, I., Cao, J., Ullah, W., Abbas, H., Ullah, S., & Zhou, J. (2023). Spatiotemporal Precipitation Trends and Associated Large-Scale Teleconnections in Northern Pakistan. *Atmosphere*, *15*, 871. https://doi.org/10.3390/atmos14050871
Rentschler, J., Salhab, M., & Jafino, B. A. (2022). Flood exposure and poverty in 188 countries. *Nat Commun*, *13*(1), 3527. https://doi.org/10.1038/s41467-022-30727-4
Rouse, J. W., Haas, R. H., Schell, J. A., & Deering, D. W. (1973). Monitoring vegetation systems in the great plains with ERTS.

Saeed, M., Li, H., Ullah, S., Rahman, A.-u., Ali, A., Khan, R., Hassan, W., Munir, I., & Alam, S. (2021). Flood Hazard Zonation Using an Artificial Neural Network Model: A Case Study of Kabul River Basin, Pakistan. *Sustainability*, *13*(24), 13953. https://www.mdpi.com/2071-1050/13/24/13953

Sakurai, M., & Murayama, Y. (2019). Information technologies and disaster management–Benefits and issues. *Progress in Disaster Science*, *2*, 100012.

Samanta, S., Pal, D. K., & Palsamanta, B. (2018). Flood susceptibility analysis through remote sensing, GIS and frequency ratio model. *Applied Water Science*, *8*(2), 66. https://doi.org/10.1007/s13201-018-0710-1

Sarhadi, A., Soltani, S., & Modarres, R. (2012). Probabilistic flood inundation mapping of ungauged rivers: Linking GIS techniques and frequency analysis. *Journal of Hydrology*, *458-459*, 68-86. https://doi.org/https://doi.org/10.1016/j.jhydrol.2012.06.039

Sarkar, D., & Mondal, P. (2019). Flood vulnerability mapping using frequency ratio (FR) model: a case study on Kulik river basin, Indo-Bangladesh Barind region. *Applied Water Science*, *10*(1), 17. https://doi.org/10.1007/s13201-019-1102-x

Shah, A. A., Ullah, A., Khan, N. A., Shah, M. H., Ahmed, R., Hassan, S. T., Tariq, M. A. U. R., & Xu, C. (2023). Identifying obstacles encountered at different stages of the disaster management cycle (DMC) and its implications for rural flooding in Pakistan [Original Research]. *Frontiers in Environmental Science*, *11*. https://doi.org/10.3389/fenvs.2023.1088126

Shen, L., Wen, J., Zhang, Y., Ullah, S., Cheng, J., & Meng, X. (2022). Changes in population exposure to extreme precipitation in the Yangtze River Delta, China. *Climate Services*, *27*, 100317. https://doi.org/https://doi.org/10.1016/j.cliser.2022.100317

Taloor, A. K., Kumar, V., Singh, V. K., Singh, A. K., Kale, R. V., Sharma, R., Khajuria, V., Raina, G., Kouser, B., & Chowdhary, N. H. (2020). Land use land cover dynamics using remote sensing and GIS Techniques in Western Doon Valley, Uttarakhand, India. *Geoecology of landscape dynamics*, 37-51.

Tariq, A., Mumtaz, F., Majeed, M., & Zeng, X. (2022). Spatio-temporal assessment of land use land cover based on trajectories and cellular automata Markov modelling and its impact on land surface temperature of Lahore district Pakistan. *Environmental Monitoring and Assessment*, *195*(1), 114. https://doi.org/10.1007/s10661-022-10738-w

Tsering, K., Shrestha, M., Shakya, K., Bajracharya, B., Matin, M., Lozano, J. L. S., Nelson, J., Wangchuk, T., Parajuli, B., & Bhuyan, M. A. (2022). Verification of two hydrological models for real-time flood forecasting in the Hindu Kush Himalaya (HKH) region. *Natural Hazards*, *110*(3), 1821-1845. https://doi.org/10.1007/s11069-021-05014-y

Uddin, K., Gurung, D. R., Giriraj, A., & Shrestha, B. (2013). Application of Remote Sensing and GIS for Flood Hazard Management: A Case Study from Sindh Province, Pakistan. *American Journal of Geographic Information System*, *2013*, 1-5. https://doi.org/10.5923/j.ajgis.20130201.01

Uddin, K., Matin, M. A., & Thapa, R. B. (2021). Rapid Flood Mapping Using Multi-temporal SAR Images: An Example from Bangladesh. *A Decade of Experience from SERVIR*, 201.

Ullah, F., Ali Shah, S. A., Saqib, S. E., Yaseen, M., & Haider, M. S. (2021). Households' flood vulnerability and adaptation: Empirical evidence from mountainous regions of Pakistan. *International Journal of Disaster Risk Reduction*, *52*, 101967. https://doi.org/https://doi.org/10.1016/j.ijdrr.2020.101967

Ullah, S., Liu, S., Adnan, M., Ashraf, M., Zaman, D. M., Hashim, S., & Muhammad, S. (2020). Risks of Glaciers Lakes Outburst Flood along China Pakistan Economic Corridor. In (pp. 1-17). https://doi.org/10.5772/intechopen.93459

UNDRR. (2020). *Human cost of disasters: An Overview of the Last 20 Years (2000-2019)*. The Centre for Research on the Epidemiology of Disasters (CRED.

USGS. (2019). *United States Geological Society*. https://www.usgs.gov/landsat-missions/landsat-normalized-difference-vegetation-index

Verpoorter, C., Kutser, T., & Tranvik, L. (2012). Automated mapping of water bodies using Landsat multispectral data. *Limnology and Oceanography: Methods*, *10*(12), 1037-1050. https://doi.org/https://doi.org/10.4319/lom.2012.10.1037

Wattanachareekul, P., Choowong, N., Pailoplee, S., & Choowong, M. (2023). Resilience to unusual flooding after 2021 tropical storms in part of mainland Southeast Asia. *Frontiers in Ecology and Evolution*, *10*, 1072993. https://doi.org/10.3389/fevo.2022.1072993

Xu, C., Zhang, X., Zhang, J., Chen, Y., Yami, T., & Hong, Y. (2021). Estimation of Crop Water Requirement Based on Planting Structure Extraction from Multi-Temporal MODIS EVI. *Water Resources Management*, *35*, 1-17. https://doi.org/10.1007/s11269-021-02838-y

Xu, H. (2006). Modification of normalised difference water index (NDWI) to enhance open water features in remotely sensed imagery. *International Journal of Remote Sensing*, *27*, 3025 - 3033.

Xue, F., Gao, W., Yin, C., Chen, X., Xia, Z., Lv, Y., Zhou, Y., & Wang, M. (2022). Flood Monitoring by Integrating Normalized Difference Flood Index and Probability Distribution of Water Bodies. *IEEE Journal of Selected Topics in Applied Earth Observations and Remote Sensing*, *15*, 4170-4179. https://doi.org/10.1109/JSTARS.2022.3176388

Yaqub, M., & Eren, B. (2015). Flood Causes, Consequences and Protection Measures in Pakistan[#381757]-408170. *1*, 8-16.

Yi, C.-S., Lee, J.-H., & Shim, M.-P. (2010). GIS-based distributed technique for assessing economic loss from flood damage: pre-feasibility study for the Anyang Stream Basin in Korea. *Natural Hazards*, *55*(2), 251-272. https://doi.org/10.1007/s11069-010-9524-7

Zhang, W., Furtado, K., Wu, P., Zhou, T., Chadwick, R., Marzin, C., Rostron, J., & Sexton, D. (2021). Increasing precipitation variability on daily-to-multiyear time scales in a warmer world. *Science Advances*, *7*(31), eabf8021.

Zhou, L., Zhou, Y., de Vries, W. T., Liu, Z., & Sun, H. (2024). Collective action dilemmas of sustainable natural resource management: A case study on land marketization in rural China. *Journal of Cleaner Production, 439*, 140872. https://doi.org/10.1016/j.jclepro.2024.140872

Zou, Q., Zhou, J., Zhou, C., Song, L., & Guo, J. (2013). Comprehensive flood risk assessment based on set pair analysis-variable fuzzy sets model and fuzzy AHP. *Stochastic Environmental Research and Risk Assessment*, *27*(2), 525-546. https://doi.org/10.1007/s00477-012-0598-5